Electrical Resistivity and Thermoelectric Power Measurements of Pyrite (FeS_2) in the Temperature Range, 78–300 K

[1]SYED MUNIR MEHDI RAZA NAQVI, [1]SHABANA RIZVI, [1]SYED DABIR HASAN RIZVI, [2]SYED MOHSIN RAZA, [3]NAJMA SHAMS AND [4]YASMIN RIZVI

[1]*Department of Physics, University of Karachi, Karachi-75270, Pakistan.*
[2]*Department of Physics, University of Balochistan, Quetta, Pakistan.*
[3]*Department of Applied Chemistry, University of Karachi, Karachi-75270, Pakistan.*
[4]*Geological Survey of Pakistan, Karachi, Pakistan.*

(Received 8th February 2007, revised 15th May 2007)

Summary: We studied the electrical resistivity and thermoelectric power of pyrite in the temperature range, 78-300 K. Electrical resistivity measurements show diverse transitions at different temperatures especially a semiconducting pumping transition, where semiconducti-vity sets in at 115 K. The insulator to metal transition in pyrite is referred to as shallowing of deep quantum wells. The shallowing of quantum well sets in at 158 K. At 195 K, the pyrite behaves as a pure metal. Further a comparative study of experimental thermoelectric power with theoretically estimated result is made.

Introduction

The electrical resistivity of liquid quenched amorphous alloys has been previously studied [1-3] in which methods of estimation of parameters are discussed. Use of Arrhenius plot for calculations of activation energy has indicated some thermally activated processes in metallic glasses, which would resolve the temperature dependent activation energies accompanying multiple kind of transitions [4]. We observed metal-insulator transition in iron-zirconium alloys at relatively high temperatures [5]. A new technique incorporating the differential thermal analysis was used for the estimation of enthalpy of amorphous alloys [6]. Our previous studies promoted us to study the indigenous rock minerals; pyrite (FeS_2) and chalcopyrite ($CuFeS_2$). Thin films of pyrite have been synthesized by others and pyrite is seen as new solar energy material due to its environ-mental compatibility and its very high absorption coefficient in the visible range [7]. Thermoelectric power studies are also of great importance for mate-rial characterization and application. At room tempe-rature, thermoelectric power, has been measured by some researchers, [8-15]. For synthetic pyrite thin films, the values range from ≈ 10 to 90 μVK^{-1}, [8-11], whereas for natural single crystal, ≈ 200 to -300 μVK^{-1}, [12-15]. Our earlier studies of x-ray diffract-tion (XRD) and magnetization properties of pyrite and chalcopyrite [16] show an overall paramagnetic nature of the two samples in the temperature range 77-300 K. In our present work, we have carried out measurements of the thermoelectric power and elect-rical resistivity of pyrite in the temperature range, 78-300 K. Grüneisen function [17-18] and various other parameters, (Table-1 and 2) have also been calculated using the technique employed in our previous work [3, 5, 18], on pyrite (FeS_2).

Results and Discussion

Fig. 1, shows electrical resistivity of pyrite. Fig. 2, represents the Arrhenius plot (log ρ versus $\frac{1000}{T}$) for electrical resistivity of pyrite. Figs. 3 and 4 show Grüneisen function versus temperature and the thermoelectric power of pyrite, in the temperature range 78-300 K. With Arrhenius plot the transition regions can be studied on the basis of our theory [3]. We labeled transition regions of electrical resistivity at various temperatures as shown in Fig. 1. The AB-transition shows metal to insulator with lowering temperature, BC - an insulator to metal transition with lowering temperature, CD - a metal to insulator transition with further lowering temperatures and more remarkably DEFG - a semiconducting pumping transition, where semiconductivity sets in at 115 K. The AC-transition in Fig. 1 is ascribed to metal softening due to trapping of electrons in quantum

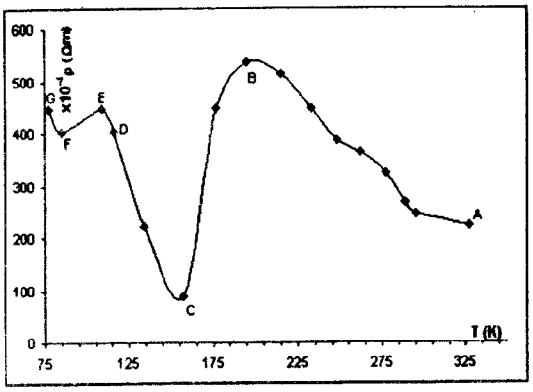

Fig. 1: Electrical Resistivity versus Temperature for Pyrite (FeS_2)

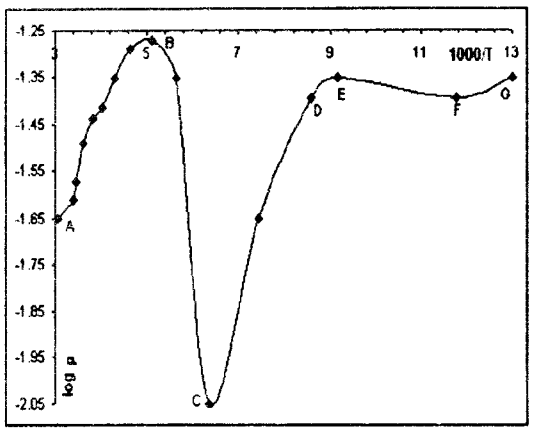

Fig. 2 Arrhenius plot for Activation Energies of Pyrite (FeS_2) i.e. log ρ vs 1000/T

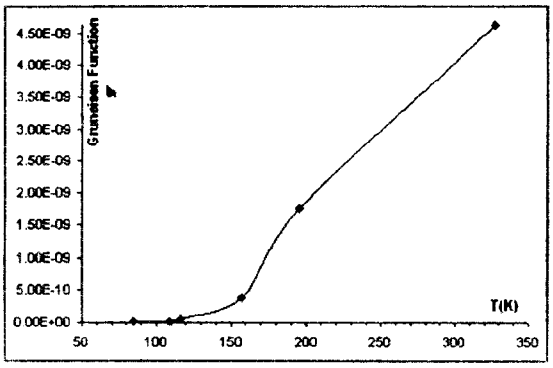

Fig. 3 Grüneisen Function versus Temperature for Pyrite (FeS_2)

wells. These transitions can be understood with the help of Arrhenius plot as shown in Fig. 2. We calculated the Bloch-Grüneisen function, $\mathscr{G}$ [17-18], by using

$$\mathscr{G} = \text{constant} \times \frac{T^5}{M\theta^6} \int_0^{\theta/T} \frac{z^5\, dz}{(e^z - 1)(1 - e^{-z})} \qquad (1)$$

Where M is the atomic weight and the constant is characteristic of the metal. We assumed a spherical Fermi-surface and neglected the Umklapp processes. Thus we are dealing with a Debye-type lattice spectrum. At high temperatures, $(T > \frac{\theta}{2})$ equation (1) reduces to

$$\mathscr{G} = \text{constant} \times \frac{T}{4M\theta^2} \qquad (2)$$

and at low temperatures ($T < \theta/10$) the upper limit of the integration in equation (1) can be taken as infinity and we may obtain

$$\mathscr{G} = \text{constant} \times \frac{124.4\ T^5}{M\,\theta^6} \qquad (3)$$

Where, the constant for each transition was calculated from Fig. 1, i.e., by employing $\frac{\Delta\rho}{\Delta T}$, θ the Debye temperature, M the atomic weight of pyrite (FeS_2), i.e., 120 amu. The Grüneisen function [17, 18] plotted in figure 3, was calculated using equation (3). Fig. 3, shows two step transitions, one at 158 K and the other at 195 K. At 158 K, the quantum wells become shallow due to which electrons overflow at the brim of walls and at 195K, the electrons become conduction electrons, as is evident from figure 3. Thus the insulator to metal transitions are referred to as shallowing of deep quantum wells.

Fig. 4 shows both theoretical and experimental results of thermoelectric power of pyrite. The thermoelectric power undulations in pyrite are decreasing with increasing temperature. We get negative thermoelectric power undulations of pyrite in the temperature range, 78-300 K. We observe experimental thermoelectric power of -25 μV/ K at temperatures 150 and 300 K, respectively. The theoretical thermoelectric power, S_{th}, is also calculated which shows a monotonic

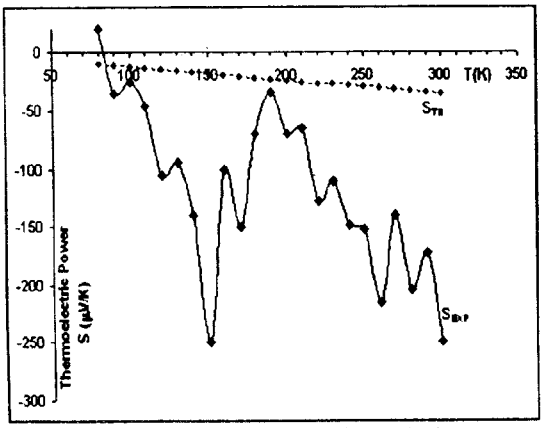

Fig. 4 Experimental and Theoretical curves showing values of Thermoelectric power (S) versus Temperature for Pyrite (FeS_2)

linear trend. There are many cases for estimating the theoretical thermoelectric power [18], but we shall restrict with diffusion thermopower for free electron, metal or alloy obeying Fermi-Dirac statistics in which $E_F >> k_BT$ (the degenerate case) and in which a single relaxation time exists. The theoretical thermoelectric power for a representative value of E_F, is given by the following equation.

$$S_{th} = -\frac{\pi^2 k_B^2 T}{3|e|E_F} \qquad (4)$$

Where, k_B is the Boltzmann constant and e is the charge of an electron. Equation (4) is valid only if mean free path is regarded as a constant. The model of constant mean free path is applicable to electron scattering by impurity atoms and equation (4) is reduced to,

$$S_{th} = -\frac{2.45\times10^{-8}T}{E_F} \qquad (5)$$

Where, E_F is in electron volts and T in Kelvin.

Tables-1 and 2 represent the calculated values and the formulae used for the parameters. The techniques used for such calculations, as mentioned in Tables-1 and 2, are taken from our previous study [3-5], excepting the Grüneisen function [17-18]. We know that sulphur, being a constituent element of pyrite, has two allotropes known as rhombic and monoclinic sulphur. Rhombic sulphur is energetically stable below 369 K. Hence, the sulphur in pyrite exists in the form of rhombic allotrope, in the temperature range, 78-300 K for electrical resistivity and thermoelectric power.

Experimental

Conventional Four Probe method [19] was employed for the electrical resistivity

Table- 1

Temperature T With Labeled Transition Regions		$\frac{\Delta\rho}{\Delta T}$	Grüneisen function	$\frac{\Delta \log \rho}{\Delta(10^3/T)}$	Activation Energy (from Arrhenius plot) with Boltzmann Constant $k_B=8.62\times10^{-5}$ eV/K	Activation Energy (from Berry)	Temperature Coefficient	Relaxation Time (from plot) with $t=7.1\times10^{-5}$s	Relaxation Time (from Berry)	Mean Free Path with $v=v_D$ $=3.41\times10^4$ ms^{-1}
		$\times10^{-4}$	$\frac{\left(\frac{\Delta\rho}{\Delta T}\right)124.4T^5}{M\theta^6}$	$\times10^{-3}$	$Q_o=\frac{\left(\frac{\Delta\log\rho}{\Delta(10^3/T)}\right)10^3 k_B}{\log e}$	$Q(T)=Q_o(1-\alpha T)$	with $t_o=10^{-13}$s $\alpha=-\left(\frac{k_B}{Q_o}\right)\log\left(\frac{t_\infty}{t_o}\right)$	$t_o=\frac{t}{\exp\left(\frac{Q_o}{k_BT}\right)}$	$t=t_o\exp\left(\frac{Q_o}{k_BT}\right)$	$l=vt_D$
(K)					(eV)	(eV)	(K^{-1})	(s)	(s)	(m)
77	G									
85	F	5.575	1.29E-11	37.38	0.007421	0.07638	-0.10933	0.000258	0.00071	8.794
109	E	1.858	1.49E-11	17.63	0.0035	0.09454	-0.23865	0.000489	0.00071	16.682
116.5	D	5.947	6.66E-11	77.35	0.015355	0.10762	-0.05157	0.000154	0.00071	5.247
157.5	C	7.633	3.86E-10	292.34	0.058035	0.16658	-0.01187	9.88E-06	0.00071	0.337
195	B	11.91	1.75E-09	637.31	0.126518	0.23716	-0.00448	3.82E-07	0.00071	0.0130
327	A	2.369	4.62E-09	183.69	0.036466	0.29831	-0.02196	0.000195	0.00071	6.640

Table- 2

Debye Wave Vector with $\frac{N}{V}=4.25\times10^{26}$ m^{-3} $k_D=\left(6\pi^2\frac{N}{V}\right)^{1/3}$	Debye Velocity with $\omega_D=10^{14}$ rad/s $v_D=\frac{\omega_D}{k_D}$	Debye Temperature with $\hbar=1.055\times10^{-34}$Js $k_B=1.38\times10^{-23}$J/K $\Theta_{theo}=\left(\frac{\hbar v_D}{k_B}\right)\left(6\pi^2\frac{N}{V}\right)^{1/3}$	Fermi Wave Vector with $\frac{N}{V}=4.25\times10^{26}$ m^{-3} $k_F=\left(3\pi^2\frac{N}{V}\right)^{1/3}$	Fermi Velocity with $\hbar=1.055\times10^{-34}$Js $m=9.11\times10^{-31}$kg $v_F=\frac{\hbar k_F}{m}$	Fermi Energy $E_F=\frac{\hbar^2k_F^2}{2m}$
(m^{-1})	(m/s)	(K)	(m^{-1})	(m/s)	(eV)
2.93×10^9	3.41×10^4	763.87	2.32×10^9	2.68×10^5	0.205

measurements on parallelepiped polished samples of pyrite. A constant current source and Keithley multimeters, 175 and 197A were used. The data were collected from 78-300 K. Thermoelectric power measurements were carried out as described elsewhere [20].

Conclusions

We infer from this study the following conclusions:

Diverse transitions at various temperatures are observed. A semiconducting pumping transition where semiconductivity sets in at 115 K. At 158K, the quantum wells in pyrite become shallow and at 195K the electrons become conduction electrons. Insulator to metal transition is referred to as shallowing of deep quantum wells.

Acknowledgement

Authors are thankful to the Higher Education Commission (HEC), for the award of the grant to carry out research work and to the Dean faculty of Science, University of Karachi, for financial support.

References

1. S. M. M. R. Naqvi, S. M. Raza, S. Dabir H. Rizvi, M. A. Gormani and N. Farooqui, *Mod. Phys. Letts. B*, 9, 195 (1995).
2. S. M. M. R. Naqvi, S. Dabir H. Rizvi, S. Jamila, S. Rizvi, S. M. Raza, M. A. Gormani and N. Farooqui, *Mod. Phys .Letts. B*, **9**, 1535 (1995).
3. M. A. Gormani, S. M. Raza, N. Farooqui, M. A. Ahmed and T. Abbas, *Solid State Commun.*, **95**, 329 (1995)
4. S. M. M. R. Naqvi, S. M. Raza, S. D. H. Rizvi, N. Shams, T. Abbas and S. M. Zia ul Haq, *Mod. Phys .Letts. B*, **5**, 1883 (1991)
5. S. M. M. R. Naqvi, S. Dabir H. Rizvi, S. M. Raza, M. A. Gormani and S. Rizvi, *Solid State Commun.* **101**, 627 (1997)
6. S. M. M. R. Naqvi, S. Dabir H. Rizvi, S. M. Raza, S. Rizvi, A. Hussain and F. Rehman, *Jour. Chem. Soc. Pak.*, **24**, 1 (2002)
7. C. Zhangqi, L. Yun, N. Mingsheng *J.Electron Devices (China)*, **20**, (4), 50 (1997).
8. J. R. Ares, M. Leon, N. M. Arozamena, J. Sanchez-Paramo, P. Celis, I. J. Ferrer and C. Sanchez, *J. Phys. Condens. Matter* **10**, 4281 (1998)
9. G.,Willeke, R. Dasbach, B. Sailer and E. Bucher, *Thin Solid Films,* **213**, 271 (1992)
10. H. Hofpner, B. Thomas, K. Ellmer B. Nippe H. Muller, H. Kerkov, A. Ennoui, S. Fiechter and H. Tributsch *12th Eur. Photovoltaic Solar Energy (Amsterdam) (Bedford: Stephens and Associates)* 1531 (1994)
11. D. Lichtenberger, K. Ellmer, R. Shieck, S. Fiechter and H. Tributsch, *Thin Solid Films,* **246**, 6 (1994)
12. D. J. Vaugham and J. R. Craig, *Mineral Chemistry of Metal Sulfides (New York, Cambridge University Press)* (1978)
13. T. M. Balesha and H. P. Dibbs *Mines Branch Technical Bulletin TB* 106 (1969)
14. P. A. Hill and R. Green, *Econom. Geol.*, **57**, 579 (1962)
15. A. Sasaki, *Mineral J,* **1,** 290 (1955)
16. S. M. M. R. Naqvi, S. Rizvi, S. Dabir. H. Rizvi, S. Z. Abbas, S. M. Raza, M. Ahmed, S. Kamaluddin and Z. Mahmood, *9th International Symposium on Advanced Materials, Proc.*, 429 (2005)
17. *'Low Temperature Physics'*, 93, by Rosenberg.
18. *'Thermoelectricity and Metals and Alloys'*, 59,127 by R. D. Barnard, Taylor and Francis, London.
19. *'Direct Current Circuits and Measurements'*, 153-155 by Charles J. Anderson, A. Santanelli and F. R. Kulis, Prentice Hall. Inc. (1966)
20. S. M. M. R. Naqvi, S. Dabir H. Rizvi, S. Fatima and S. Mohsin Raza, *Mod. Phys. Letts. B*, 7, 1331 (1993).